PRELIMINARY EVALUATION OF HYDROLOGIC PROPERTIES OF CORES OF UNSATURATED TUFF, TEST WELL USW H-1, YUCCA MOUNTAIN, NEVADA

By E. P. Weeks and William E. Wilson

U.S. GEOLOGICAL SURVEY

Water-Resources Investigations Report 84-4193

Prepared in cooperation with the

U.S. DEPARTMENT OF ENERGY

Denver, Colorado
1984

UNITED STATES DEPARTMENT OF THE INTERIOR

WILLIAM P. CLARK, SECRETARY

GEOLOGICAL SURVEY

Dallas L. Peck, Director

For additional information
write to:

Chief, Nuclear Hydrology Program
Water Resources Division,
U.S. Geological Survey
Box 25046, Mail Stop 416
Denver Federal Center
Lakewood, CO 80225

Copies of this report
can be purchased from:

Open-File Services Section
Western Distribution Branch
U.S. Geological Survey
Box 25425, Federal Center
Lakewood, CO 80225
[Telephone: (303) 236-7476]

CONTENTS

ILLUSTRATIONS

TABLE

METRIC CONVERSION TABLE

For those readers who prefer to use inch-pound rather than metric units, conversion factors for the terms used in this report are listed below:

Metric unit	*Multiply by*	*To obtain inch-pound unit*
centimeter	3.937×10^{-1}	inch
meter (m)	3.281	foot
kilometer	6.214×10^{-1}	mile
cubic centimeter (cm^3)	6.102×10^{-2}	cubic inch
gram per cubic centimeter (g/cm^3)	6.243×10^{1}	pound per cubic foot
centimeter per second (cm/s)	1.367×10^{-3}	foot per day
centimeter per second squared	3.281×10^{-2}	foot per second squared
millimeter per year (mm/yr)	3.937×10^{-2}	inch per year
dyne per centimeter (dyne/cm)	5.71×10^{-6}	pound per inch
kilopascal	1.00×10^{-2}	bar
	1.45×10^{-1}	pound per square inch
centimeter of water	9.80×10^{-4}	bar
centimeter of mercury	1.934×10^{-1}	pound per square inch
	1.33×10^{-2}	bar
degree Celsius (°C)	F=9/5°C+32	degree Fahrenheit (°F)

PRELIMINARY EVALUATION OF HYDROLOGIC PROPERTIES OF CORES OF UNSATURATED TUFF, TEST WELL USW H-1, YUCCA MOUNTAIN, NEVADA

By E. P. Weeks and William E. Wilson

ABSTRACT

The unsaturated zone at Yucca Mountain, Nevada, is being evaluated as a potential repository for high-level nuclear wastes. Estimates of ambient moisture tension, effective hydraulic conductivity, and vertical flux are needed to design additional investigations and to develop preliminary models of the geohydrologic system. In deep unsaturated zones of uniform properties, hydraulic-head gradients are unity, and effective hydraulic conductivity may be used to estimate vertical flux.

Analyses were made on 19 core samples of unsaturated tuff from test well USW H-1. Moisture-characteristic curves relating saturation and moisture tension were developed from results of mercury-injection tests. Ambient moisture tension estimated from these curves generally was 100 to 200 kilopascals. Values of relative permeability ranging from about 0.002 to 0.1 were determined by fitting an analytical expression to eight of the moisture-characteristic curves, and then integrating to solve for relative permeability. These values of relative permeability were applied to values of saturated hydraulic conductivity of core from a nearby test well to obtain effective hydraulic conductivities of about 8×10^{-12} to 7×10^{-10} centimeter per second. If a unit hydraulic-head gradient is assumed, these values convert to a vertical flux through the tulf matrix of 0.003 to 0.2 millimeter per year. The validity of this assumption was not verified due to the sparseness of data and uncertainties in their reliability. Consequently, the results of this study are preliminary and need to be used only as a guide for future studies.

INTRODUCTION

Background

Unsaturated tuff underlying Yucca Mountain, Nevada Test Site and vicinity, is being evaluated for its suitability as a host medium for storing high-level radioactive wastes. One reason for considering this medium is the presumed low flux of water through the unsaturated section. Estimates of moisture tension and effective hydraulic conductivity under ambient conditions of moisture content (or saturation) are needed to make preliminary estimates of matrix flux and to design additional experiments to refine the estimates. The information contained in this report was obtained as part of the Nevada Nuclear Waste Storage Investigations being made in part by the U.S. Geological Survey in cooperation with the U.S. Department of Energy under Interagency Agreement DE-AI08-78ET44802.

In unsaturated zones that are hundreds of meters thick, the large near-surface fluctuations in soil-moisture tension that result from episodic infiltration events followed by evapotranspiration become totally dampened at depth, and deep percolation becomes nearly constant with time. Consequently, the average vertical flux can be estimated if measurements are available of the hydraulic-head gradient and of the effective hydraulic conductivity at the prevailing moisture content or moisture tension. Moreover, if the materials in the unsaturated zone have uniform hydraulic properties with depth, the total hydraulic-head gradient is unity (fig. 1), and the vertical flux may be computed from Darcy's law for unsaturated flow:

$$q = K(\Psi) \frac{d\Psi}{dZ}$$

If the hydraulic-head gradient is unity ($\frac{d\Psi}{dZ} = 1$), the equation becomes:

$$q = K(\Psi) \ , \qquad (1)$$

where q is the downward vertical flux of water, L/T;
$K(\Psi)$ is the vertical hydraulic conductivity at the prevailing moisture tension, or the effective hydraulic conductivity, L/T; and
Ψ is the moisture tension, defined as negative pressure head, L.

Thus, in thick, uniform unsaturated zones, the average vertical flux can be estimated from a few measurements of effective hydraulic conductivity (Jacob Rubin, U.S. Geological Survey, written commun., 1977).

Most thick unsaturated zones are not uniform, but consist of layered units of differing properties. Under these conditions, percolation is steady at great depths, but a separate moisture-content or saturation profile occurs within each unit, as shown in figure 2 (Childs, 1969, p. 230). Moisture contents are discontinuous at unit boundaries, but if the units are thick enough, the moisture contents become nearly uniform at some distance from the lower boundary within each unit. By inference, the moisture tension within the part of each unit unaffected by the unit boundary also would be relatively uniform, indicating a gradient of total hydraulic head near unity. Under these conditions, vertical flux could be computed by applying equation 1 to data obtained from individual units, as long as the data were not obtained from parts of the unit affected by boundary conditions.

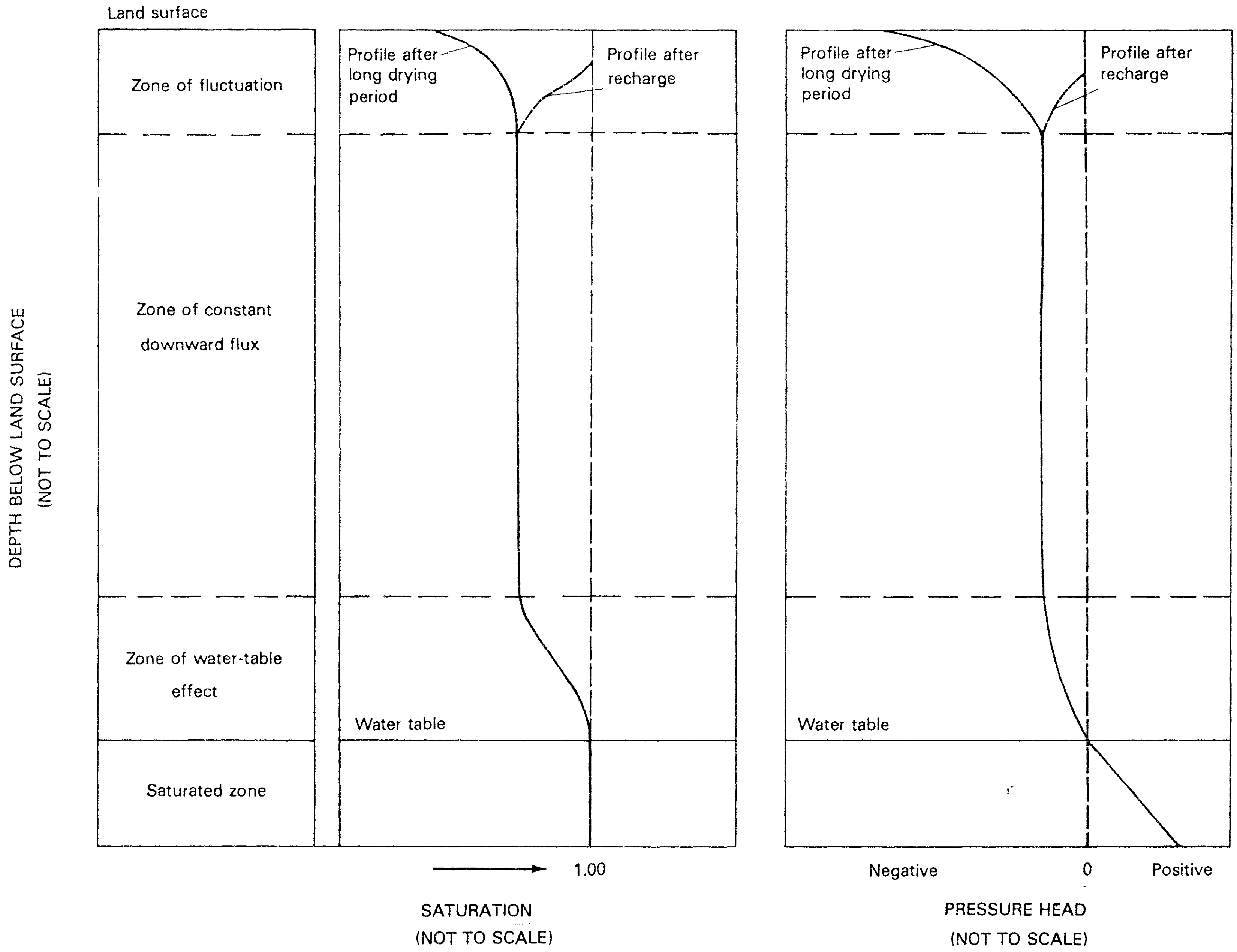

Figure 1.--Conceptual model of unsaturated flow through thick, uniform porous media.

CORRECTED FIGURE 2; PLEASE SUBSTITUTE FOR FIGURE 2 IN PRINTED REPORT

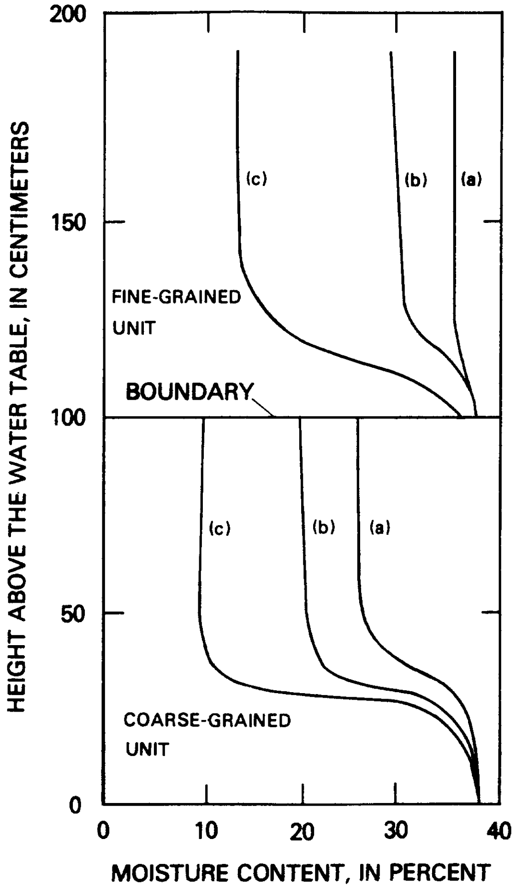

(a), downward vertical flux = 9.9 centimeters per minute;
(b), downward vertical flux = 0.35 centimeter per minute;
(c), downward vertical flux = 0.035 centimeter per minute

Figure 2.--Moisture-content profiles during steady percolation in layered media consisting of finer-grained materials overlying coarser-grained materials (modified from Childs, 1969, fig. 12.7).

Yucca Mountain is underlain by a thick, nonuniform unsaturated zone. Depth to water ranges from about 300 to about 750 m below land surface (Robison, 1984). The section of unsaturated tuff has been divided into hydrogeologic units, based principally on the degree of welding (Scott and others, 1983; Parviz Montazer and W.E. Wilson, U.S. Geological Survey, written commun., 1984). These units, which are tens to hundreds of meters thick, differ substantially in their physical and hydraulic properties, including fracture density, porosity, moisture content, and saturated hydraulic conductivity (Anderson, 1981; Scott and others, 1983; Parviz Montazer and W.E. Wilson, written commun., 1984). The thickness of some of the hydrogeologic units at Yucca Mountain may be sufficiently great and the hydraulic properties within those units sufficiently uniform that vertical flux through the tuff matrix could be computed from the effective matrix hydraulic conductivity of such a unit.

Purpose and Scope

This report presents estimates of ambient moisture tension and effective hydraulic conductivity of the tuff matrix at Yucca Mountain. These data are needed to design experiments and select instrumentation for additional studies to characterize the hydrology of the proposed repository site. In addition, the estimates are used in this report to make a preliminary estimate of vertical matrix flux at Yucca Mountain, and a qualitative assessment is made of the applicability of this method for this site. Preliminary estimates of vertical flux are needed for development of conceptual geohydrologic models and preliminary flow models of the unsaturated zone.

The early hydrologic test drilling program at Yucca Mountain was designed to evaluate the suitability of the saturated zone as a repository medium. Consequently, although cores were collected from the unsaturated zone, no direct measurements were made of moisture tension and hydraulic conductivity at ambient moisture content. However, mercury-porosimetry tests were made on selected cores from test well USW H-1, and results of these tests form the basis of the analysis presented in this report. The approach used was to combine the porosimetry data with existing data on ambient moisture content to estimate moisture tension and relative hydraulic conductivity. Values of relative hydraulic conductivity were applied to measurements of saturated hydraulic conductivity previously made on cores of the same geologic units from a nearby corehole, to estimate effective matrix hydraulic conductivity and vertical water flux in the tuff matrix.

Because of the uncertainties in the reliability of some of the data and in the appropriateness of applying equation 1 to the conditions at Yucca Mountain, the results presented in this report are considered preliminary and need to be used principally as guidelines for further investigations.

TEST-WELL AND CORE DATA

Test well USW H-1 was drilled at Yucca Mountain, near the western border of the Nevada Test Site (fig. 3), to a depth of 1,829 m below land surface; depth to the composite static water level was 752 m. Detailed data concerning laboratory analyses of core, well construction, and hydraulic testing are presented in a report by Rush and others (1983). Although the test well was drilled primarily to obtain hydrologic information concerning tuff in the saturated zone, cores were collected at selected intervals throughout both the unsaturated and saturated parts of the section. The well was drilled using an air-foam mixture, and the cores were waxed and sealed after retrieval.

Laboratory analyses were made on selected cores from the unsaturated zone (Rush and others, 1983). In addition, small samples were taken from some of these cores for use in mercury-injection (porosimetry) tests made by Holmes and Narver, Inc., a contractor for the U.S. Department of Energy. Depths, hydrogeologic units, and selected characteristics for these samples are summarized in table 1; data are tabulated for 19 samples collected at depths ranging from 34 to 533 m.

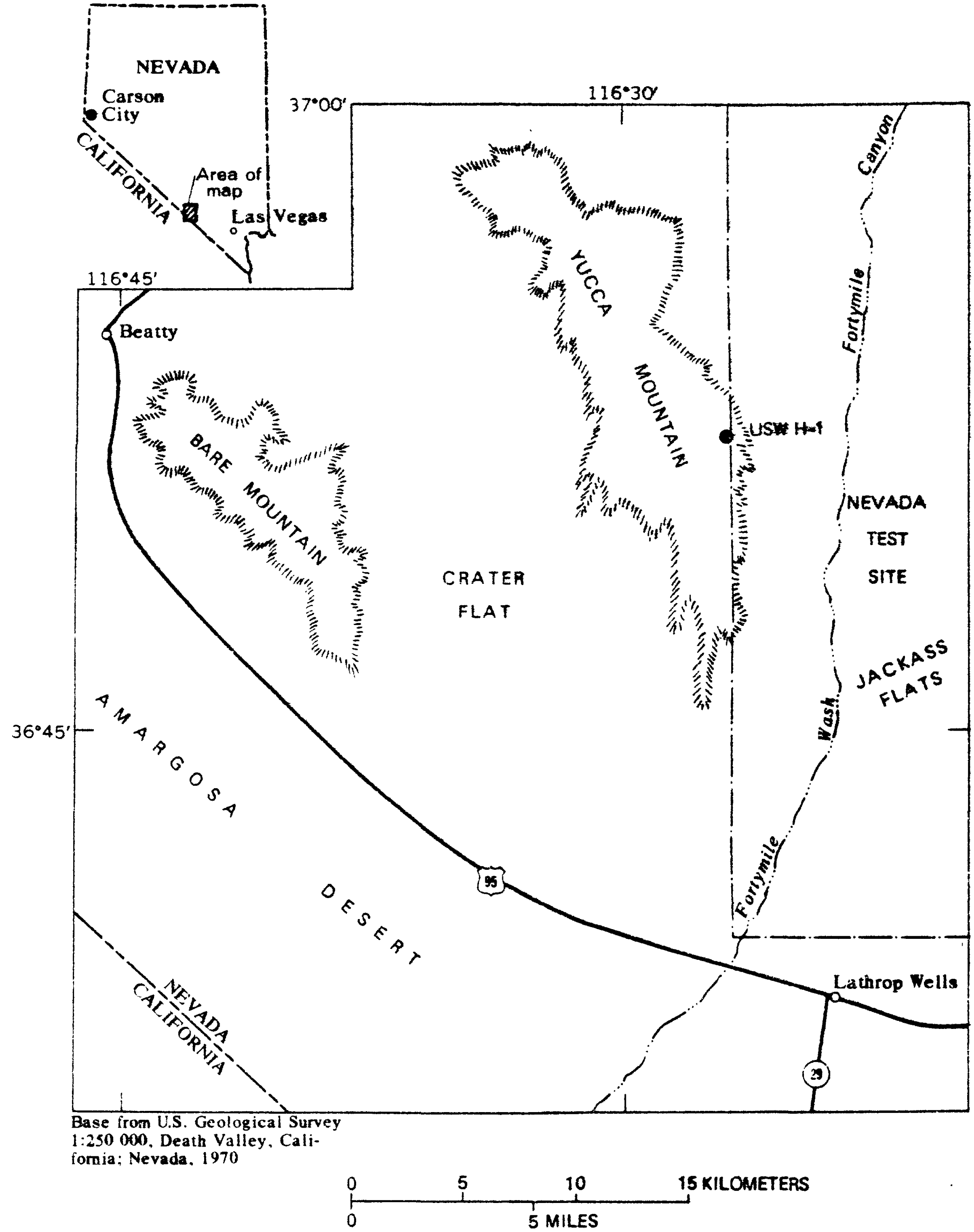

Figure 3.--Location of test well USW H-1.

Table 1.--*Characteristics of core samples from the unsaturated zone, test well USW H-1*

[m, meters; g/cm³, grams per cubic centimeter; cm³/cm³, cubic centimeters per cubic centimeter; kPa, kilopascal]

Sample number	Depth below land surface (m)	Hydrogeologic unit	Density (g/cm³)		Porosity, Ø[3] (cm³/cm³)		Volumetric moisture content[2] (cm³/cm³)
			Dry bulk[1]	Grain[2]	Large sample[2]	Sub-sample[1]	
1	33.5	Paintbrush nonwelded unit	1.38	2.40	0.446	0.428	0.220
2	128.0		2.07	2.60	.215	.205	.096
3	129.1		2.08	2.60	.232	.197	.113
4	134.9		2.07	2.60	.210	.201	.093
5	136.6		2.14	2.59	.189	.174	.107
6	142.5		2.18	2.58	.168	.155	.090
7	143.3		2.23	2.57	.149	.130	.085
8	219.2	Topopah Spring	2.17	2.55	.173	.149	.127
9	221.4	welded unit	2.09	2.56	.278	.183	.118
10	222.1		2.19	2.56	.176	.143	.120
11	225.6		2.16	2.54	-----	.151	.115
12	390.4		2.16	2.56	.159	.156	.111
13	390.6		2.21	2.56	.155	.140	.114
14	397.9		2.28	2.58	.141	.117	.102
15	398.7		2.31	2.59	.103	.109	.082
16	405.4		2.28	2.58	-----	.177	.104
17	405.8		2.35	2.59	-----	.095	.084
18	530.7	Calico Hills	1.30	2.41	-----	.461	.459
19	532.8	nonwelded unit	1.43	2.47	-----	.409	.422

Sample number	Matrix saturation, s[4]	Ambient moisture tension, ψ[5] (kPa)	λ[6]	Moisture tension at at maximum capillary rise, ψ_c[6] (kPa)	Relative hydraulic conductivity, K_w, at inferred moisture tension, ψ[7] (dimensionless)
1	0.51	150	0.32	20	0.003
2	.47	190	.50	43	.007
3	.57	120	.38	32	.010
4	.46	230e	.36	34	.002
5	.61	180	----	----	-----
6	.58	250e	----	----	-----
7	.65	180	----	----	-----
8	.85	70	.23	40	.200
9	.64	230e	.21	29	.005
10	.84	70	.22	34	.100
11	.73	100	.25	29	.040
12	.71	170	----	----	-----
13	.81	140	----	----	-----
14	.87	>250	----	----	-----
15	.75	>250	----	----	-----
16	.89	220e	----	----	-----
17	.88	>250	----	----	-----
18	1.00	<10	----	----	-----
19	>1	-----	----	----	-----

[1]Analyses made on subsamples used for mercury-injection tests.

[2]From Rush and others (1983).

[3]Porosity = one - bulk density/grain density.

[4]Saturation = volumetric moisture content/porosity of subsample.

[5]From moisture-characteristic curves (figs. 4-22 in Supplemental Data section at the end of the report); e, estimated from extension of curves.

[6]From log-log moisture-characteristic plots (figs. 23-30 in Supplemental Data section at the end of the report).

[7]Computed from the formulation of Brooks and Corey (1964).

METHODS AND RESULTS OF ANALYSIS

Mercury-Injection Tests

Mercury-injection tests were made on cores from the unsaturated zone at test well USW H-1, and the data were used to develop moisture-characteristic curves relating matrix saturation and moisture tension. The tests were conducted by placing a small sample in a porosimeter chamber, evacuating air from the chamber with a vacuum pump, and then injecting mercury into the sample under several step increases in pressure. After each step increase in pressure, the volume of injected mercury was allowed to equilibrate with time and then measured.

Both the matrix saturation to mercury and the applied mercury-injection pressures need to be manipulated to determine equivalent matrix saturation to water and equivalent moisture tension. The equivalent matrix saturation to water for a given volume of mercury injection is equal to the complement of the matrix saturation to mercury, because mercury, like air, is a nonwetting fluid:

$$s = (V_\theta - V_{Hg}) / V_\theta \qquad (2)$$

where s is matrix saturation to water, dimensionless;

V_θ is volume of pore space, in cubic centimeters; and

V_{Hg} is volume of injected mercury, in cubic centimeters.

The equivalent moisture tension for a given mercury-injection pressure was determined from the capillary-rise law (Stallman, 1964):

$$H_L = \frac{2\tau_{L-G} \cos\alpha_{L-S}}{\rho_L \, gr} \qquad (3)$$

where H_L is the height of capillary rise of liquid, L, in centimeters;

τ_{L-G} is surface tension of liquid, L, against gas, G, in dynes per centimeter;

α_{L-S} is contact angle of liquid, L, against the solid surface, S, as measured through the liquid, in degrees;

ρ_L is density of liquid, in grams per cubic centimeter;

g is acceleration due to gravity, in centimeters per second squared; and

r is radius of capillary, in centimeters.

From this principle,

$$\frac{H_w}{H_{Hg}} = \frac{\rho_{Hg}}{\rho_w} \frac{\tau_{w-A}}{\tau_{Hg-V}} \frac{\cos\alpha_{w-S}}{\cos\alpha_{Hg-S}} \tag{4}$$

where ρ_{Hg} is 13.56 g/cm³;

ρ_w is 1.00 g/cm³;

τ_{w-A} is 73 dynes/cm (20°C);

τ_{Hg-V} is 480 dynes/cm (20°C);

α_{w-S} is 0°;

α_{Hg-S} is 140°;

subscript A is air; and
subscript V is vacuum.

Hence, $\frac{H_w}{H_{Hg}} = 2.69$, or a pressure head of 1 cm of mercury is equivalent to a moisture tension of 2.69 cm of water.

Moisture-Characteristic Curves

Curves showing the relationship between volumetric moisture content or matrix saturation and moisture tension, commonly called moisture-characteristic curves, were used to estimate moisture tensions from moisture-content measurements. Moisture-characteristic curves were prepared from results of the mercury-injection tests by: (1) Plotting the computed matrix saturation (eq. 2) versus the inferred moisture tension that was equivalent to the applied mercury-injection pressure for that step, and (2) connecting the points by line segments. Moisture-characteristic curves are shown in the Supplemental Data section at the end of the report (figs. 4-22).

Ambient Moisture Tension

Ambient moisture tensions were estimated first by computing ambient matrix saturations from the volumetric moisture contents and porosity of the samples, and then by selecting the moisture tensions that correspond to those matrix saturations on the moisture-characteristic curves.

Volumetric moisture content was determined for each interval from the entire core sample. Porosity was determined from both the entire core sample (table 1, large sample) and the subsample used in the mercury-injection tests (table 1, subsample). Both porosity values were computed from the dry-bulk density and grain density of the appropriate samples by the equation:

$$\emptyset = 1 - \frac{\rho_b}{\rho_g} \qquad (5)$$

where $\emptyset$ is porosity, dimensionless;
ρ_b is dry bulk density, g/cm^3; and
ρ_g is grain density, g/cm^3.

The subsample values of porosity are the ones that were used in the calculation of ambient matrix saturations. The calculated matrix saturations range from 0.46 to more than 1.0 (table 1).

Some error may have been introduced by using the subsample to determine the moisture-characteristic curve and porosity, while using the large sample to obtain volumetric moisture content. As shown in table 1, the porosities of the subsamples generally are slightly smaller than those for the large samples. The differences possibly are due to fractures in the large samples that were absent in the subsamples. Other possible sources of error include wetting of the sample during drilling and drying of the sample prior to wrapping and waxing after the core was collected.

Selection of the ambient moisture tensions from the moisture-characteristic curves was not always straightforward. The porosimetry data were collected only to a pressure of 1,000 kPa (kilopascals), which is equivalent to a water tension of about 200 kPa. Pore sizes for all the samples were extremely small, and, as a consequence, the curves are incomplete and generally extend only to a matrix saturation slightly less than the ambient volumetric moisture content. Some ambient matrix saturations were less than the minimum value determined by mercury injection and for these samples the moisture tensions had to be estimated by extrapolation. Matrix saturations for four samples either were so small that no extrapolation could be made, or were so large that no meaningful values could be estimated.

Ambient moisture tensions were determined for 14 samples; values ranged from less than 10 to more than 250 kPa, with a mean of 160 ± 60 kPa (table 1). As mentioned above, the cores may have been wetted by the liquid in the air foam used for drilling, or they may have dried somewhat before being wrapped and waxed. In general, if the true ambient matrix saturations were 0.1 greater or less than those measured on the cores, the actual moisture tensions would be 50 to 100 kPa less or greater than determined. Taking into account these probable sources of error, the mean *in situ* moisture tensions in the intervals tested could be as small as 60 kPa or as great as 260 kPa.

Relative Hydraulic Conductivity

Relative hydraulic conductivity, K_r, defined as the ratio of hydraulic conductivity at a given matrix saturation to that at complete matrix saturation, can be estimated from moisture-characteristic curves. Two methods, both based on capillary-tube-bundle models, were considered for this study. One method involves the analysis of the moisture-characteristic curve as a series of discrete intervals, as described, for example, by Green and Corey (1971). This method could not be applied in this study because the moisture-tension data do not extend to a large enough range to provide nearly complete curves, a requirement of the method.

The second approach involves fitting an analytical expression to the moisture-characteristic curve, which then can be integrated to give an equation for relative permeability as a function of matrix saturation or moisture tension. Moisture-characteristic curves from eight samples could be fit by the Brooks-Corey (1964) equation:

$$s_e = (\Psi/\Psi_c)^{-\lambda} \qquad (6)$$

where s_e is effective matrix saturation, defined as $\frac{s-s_r}{1-s_r}$, dimensionless;

s is total matrix saturation, dimensionless;
s_r is residual or irreducible matrix saturation, dimensionless;
Ψ is moisture tension of interest, cm of water;
Ψ_c is moisture tension at the maximum capillary rise (actually a fitting parameter), cm of water; and
λ is an exponent characterizing pore-size distribution, dimensionless.

This formulation requires the identification of three fitting parameters: λ, Ψ_c, and s_r. The λ and Ψ_c terms were determined by fitting a straight line through a log-log plot of Ψ versus s_e. For λ, two points were selected on the straight line with coordinates of s_{e_1}, Ψ_1 and s_{e_2}, Ψ_2. These were substituted in the equation:

$$\lambda = \frac{\log s_{e_2} - \log s_{e_1}}{\log \Psi_2 - \log \Psi_1}$$

A value for Ψ_c is the intercept of the extrapolated straight line at $s_e = 1$. The residual matrix saturation, s_r, was estimated by: (1) A manual trial-and-error substitution to produce the straightest line on the log-log plot; and (2) an automatic search procedure to find the value of s_r that minimizes the sum-of-square residual between the best-fit straight line and the data (Mualem, 1976). Both methods yielded s_r values that equal about zero.

Theoretically, the residual matrix saturation represents the minimum saturation that can be obtained by drainage. However, in this application, residual matrix saturation is merely a curve-fitting parameter that linearizes the log-log moisture-characteristic plot. The s_r values determined for this study are particularly lacking in physical significance because they were determined from substantially incomplete moisture-characteristic curves.

Log-log plots of Ψ versus s_e for the eight samples that could be analyzed are shown in the Supplemental Data section at the end of the report (figs. 23-30); values for λ and Ψ_c are listed in table 1.

Data from 11 samples failed to fit the Brooks-Corey model. Moisture-characteristic curves generally are S-shaped, concave downward at the wet ends and concave upward at the dry ends. For the eight tuff samples for which analysis was possible, only a small proportion of the pore space occurs in the downward-concave part of the curve, which is ignored in the Brooks-Corey model. However, for 11 of the samples, the downward-concave part of the curve occupied the entire part of the determined pore-size distribution curve, and no fit was possible. In fact, these curves included only a small part of the entire moisture-characteristic curve, because most of the pores were too small to be sampled by the 1,000 kPa mercury-injection pressure. Therefore, for these 11 samples, data are inadequate for determination of relative hydraulic conductivity.

Relative hydraulic conductivity was computed from λ and Ψ_c by the following equation (Mualem, 1976, as modified from Brooks and Corey, 1964):

$$K_r = (\Psi/\Psi_c)^{-2-\lambda(2+n)} \qquad (8)$$

The parameter n has been assigned values ranging from 0 to 2 by various investigators. Mualem (1976) observed that, overall, a value of 0.5 gives the best match between computed and measured relative hydraulic conductivities for a large group of samples reported in the literature; this value was used to compute the relative hydraulic conductivities in this report.

Relative hydraulic conductivities at the inferred moisture tension for the eight analyzable samples were computed by inserting the inferred moisture tension, along with appropriate values for λ and Ψ_c, into equation 8. The dimensionless relative hydraulic conductivities, listed in table 1, range from 0.002 to 0.2. The 0.2 value probably is unreliable because the porosity of the total sample was much larger than that of the small sample used in the porosimeter. The geometric mean of the seven values of relative hydraulic conductivity considered valid is 0.01, and the median is 0.007.

Effective Hydraulic Conductivity and Vertical Flux

Effective hydraulic conductivity, or ambient unsaturated hydraulic conductivity, may be estimated from the relative hydraulic conductivity if the saturated hydraulic conductivity is known. No measurements of saturated hydraulic conductivity were made on the cores from the unsaturated zone penetrated by test well USW H-1. However, permeability measurements, using water as the test fluid, were obtained by Anderson (1981) on 16 cores of the Topopah Spring Member of the Paintbrush Tuff from test well UE25a#1, located 2.0 km east of test well USW H-1. Anderson presents maximum and minimum permeability values for some samples and single values for others. He also discounts the results of one core analysis because of a visible fracture. The geometric mean of saturated hydraulic conductivity of the minimum or single values for the other 15 samples is 4×10^{-9} cm/s, and that for the maximum values is 7×10^{-9} cm/s. Based on this range and on the range of relative hydraulic conductivities, effective hydraulic conductivities are 8×10^{-12} to 7×10^{-10} cm/s.

Assuming that a unit hydraulic gradient exists, the estimates of effective hydraulic conductivity would convert into a vertical water flux through the tuff matrix of 0.003 to 0.2 mm/yr. These values are extremely approximate because no attempt was made to relate saturated hydraulic conductivities and relative hydraulic conductivities to individual hydrogeologic units, a requirement for rigorously applying equation 1. Nonetheless, the values probably bracket the actual matrix flux through the tuffs at Yucca Mountain.

SUMMARY AND CONCLUSIONS

Analyses were made on cores of unsaturated tuff from test well USW H-1 at Yucca Mountain, Nevada, to provide preliminary estimates of ambient moisture tension, effective hydraulic conductivity, and vertical flux through the matrix. These results could be used to guide future studies. Flux analyses were based on the assumption that properties of some hydrogeologic units are sufficiently uniform that the total hydraulic-head gradient is unity, and the vertical flux, therefore, could be computed from the effective hydraulic conductivity.

Test well USW H-1 was drilled to 1,829 m. Laboratory analyses were made on 19 samples of core collected at depths ranging from about 34 to about 533 m.

Data from mercury-injection tests were used to construct moisture-characteristic curves. Ambient moisture tensions, determined from these curves, using ambient matrix saturations, ranged from less than 10 to more than 250 kPa; *in situ* moisture tensions in the intervals tested probably are 60 to 260 kPa.

Relative hydraulic conductivity ranges from 0.002 to 0.1 (dimensionless), with a geometric mean of about 0.01, based on analysis of seven of the samples. Average saturated hydraulic conductivities of 4×10^{-9} to 7×10^{-9} cm/s were obtained from laboratory analyses of 15 cores from nearby test well UE25a#1. Applying the range of relative hydraulic conductivity values results in a vertical flux (under an assumed unit hydraulic gradient) of 0.003 to 0.2 mm/yr through the tuff matrix.

The relatively narrow range of moisture tensions inferred for the Topopah Spring welded unit (generally 100-200 kPa) indicates that a hydraulic gradient of unity may prevail in this hydrogeologic unit. If so, the effective hydraulic conductivity appropriately could be used to estimate vertical flux. However, the data are sparse and unevenly distributed with depth, and uncertainties exist in their reliability. Thus, the uniformity of properties in the unit has not been demonstrated sufficiently to assess the applicability of the method used. Nevertheless, the results can be used to guide further investigations. Instrumentation for monitoring *in situ* moisture tensions should be designed to measure values of about 100 to 200 kPa, and conceptual geohydrologic models and preliminary flow models of the unsaturated zone should accommodate a very low flux in the tuff matrix.

REFERENCES CITED

Anderson, L.A., 1981, Rock property analysis of core samples from the Yucca Mountain UE25a-1 borehole, Nevada Test Site, Nevada: U.S. Geological Survey Open-File Report 81-1338, 40 p.

Brooks, R.H., and Corey, A.T., 1964, Hydraulic properties of porous media: Fort Collins, Colorado State University Hydrology Paper 3, 19 p.

Childs, E.C., 1969, The physical basis of soil water phenomena: New York, Wiley-Interscience, p. 230-232.

Green, R.E., and Corey, J.C., 1971, Calculation of hydraulic conductivity: A further evaluation of some predictive methods: Soil Science Society of America Proceedings, v. 35, no. 1, p. 1-8.

Mualem, Y., 1976, A new model for predicting the hydraulic conductivity of unsaturated porous media: Water Resources Research, v. 12, no. 3, p. 513-522.

Robison, J.H., 1984, Ground-water level data and preliminary potentiometric-surface maps, Yucca Mountain and vicinity, Nye County, Nevada: U.S. Geological Survey Water-Resources Investigations 84-4197, 11 p. [in press].

Rush, F.E., Thordarson, William, and Bruckheimer, Laura, 1983, Geohydrologic and drill-hole data for test well USW-H1, adjacent to Nevada Test Site, Nye County, Nevada: U.S. Geological Survey Open-File Report 83-141, 43 p.

Scott, R.B., Spengler, R.W., Diehl, S., Lappin, A.R., and Chornack, M.P., 1983, Geologic character of tuffs in the unsaturated zone at Yucca Mountain, southern Nevada, *in* Mercer, J. W., Rao, P.S.C., and Marine, I. W., eds., Role of the unsaturated zone in radioactive and hazardous waste disposal: Ann Arbor, Mich., Ann Arbor Science, p. 289-335.

Stallman, R.W., 1964, Multiphase fluids in porous media--A review of theories pertinent to hydrologic studies: U.S. Geological Survey Professional Paper 411-E, p. E1-E51.

SUPPLEMENTAL DATA: MOISTURE-CHARACTERISTIC CURVES

Moisture-characteristic curves showing the relation between saturation and moisture tension for 19 cores from test well USW H-1 are shown in figures 4-22. Graphs relating the logarithm of saturation and the logarithm of moisture tension are shown for eight of the cores in figures 23-30. See table 1 for a summary of core characteristics.

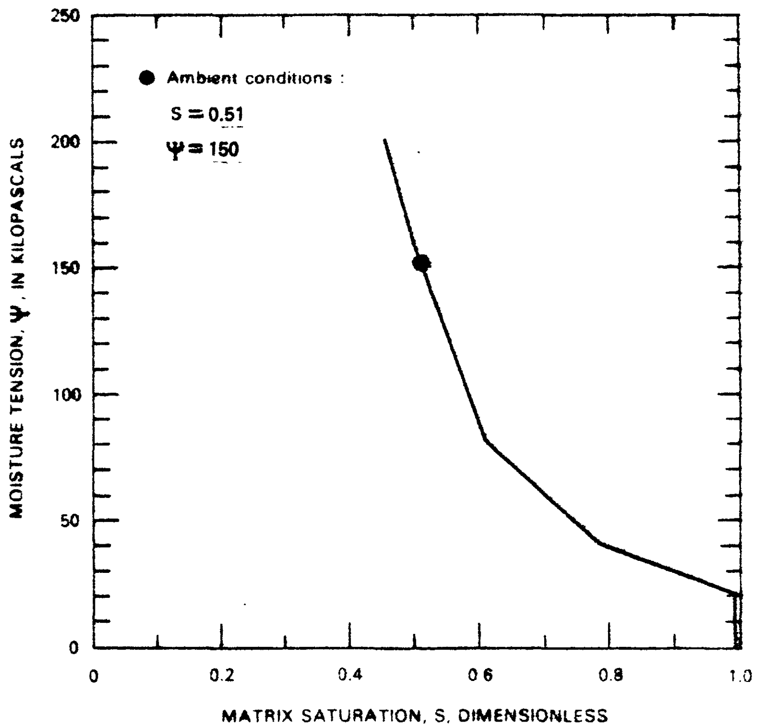

Figure 4.--Relation between matrix saturation and moisture tension, core from test well USW H-1 at a depth of 33.5 meters (sample 1).

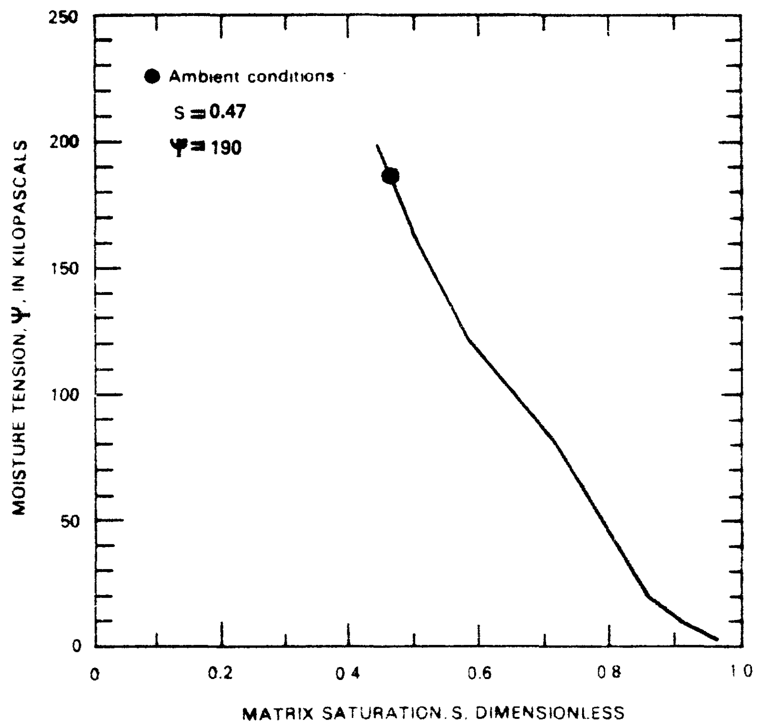

Figure 5.--Relation between saturation and moisture tension, core from test well USW H-1 at a depth of 128.0 meters (sample 2).

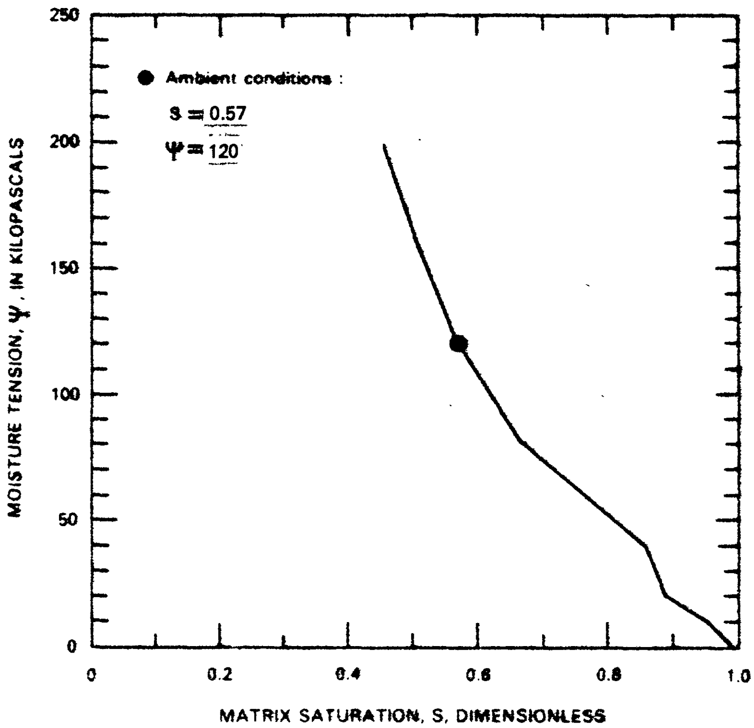

Figure 6.--Relation between saturation and moisture tension, core from test well USW H-1 at a depth of 129.1 meters (sample 3).

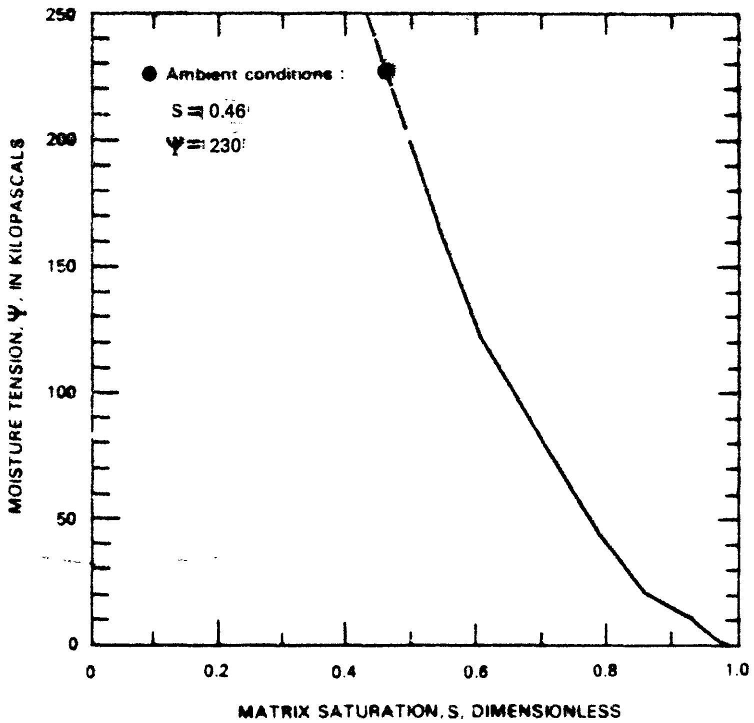

Figure 7.--Relation between saturation and moisture tension, core from test well USW H-1 at a depth of 134.9 meters (sample 4).

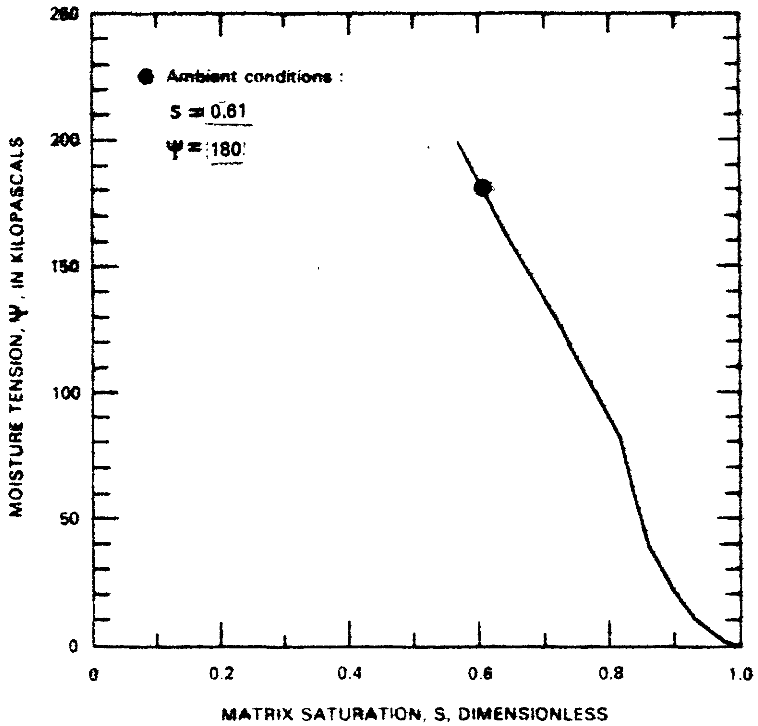

Figure 8.--Relation between saturation and moisture tension, core from test well USW H-1 at a depth of 136.6 meters (sample 5).

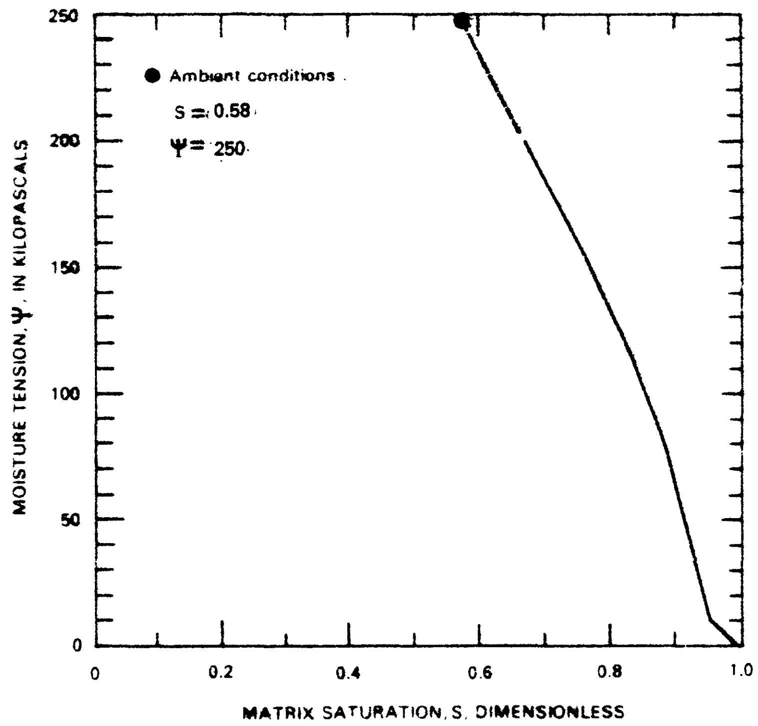

Figure 9.--Relation between saturation and moisture tension, core from test well USW H-1 at a depth of 142.5 meters (sample 6).

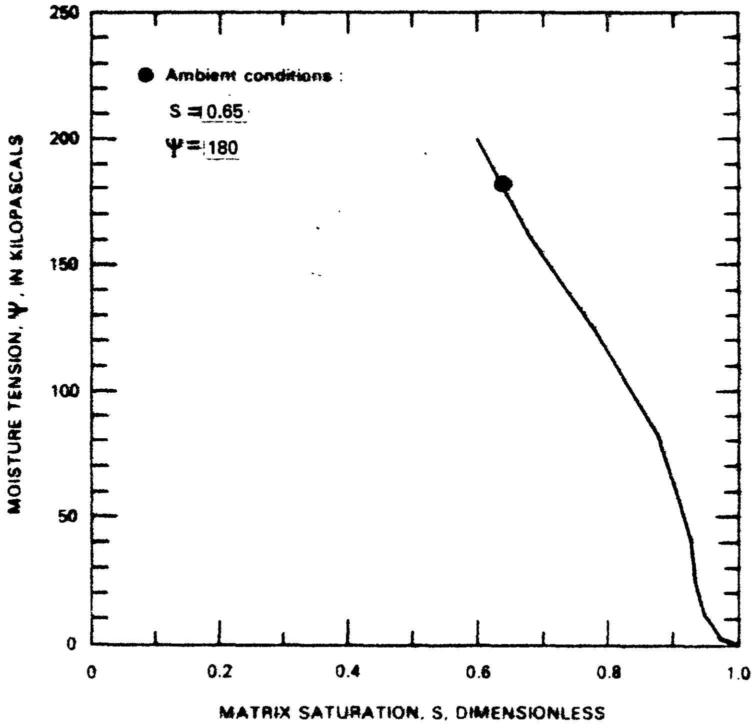

Figure 10.--Relation between saturation and moisture tension, core from test well USW H-1 at a depth of 143.3 meters (sample 7).

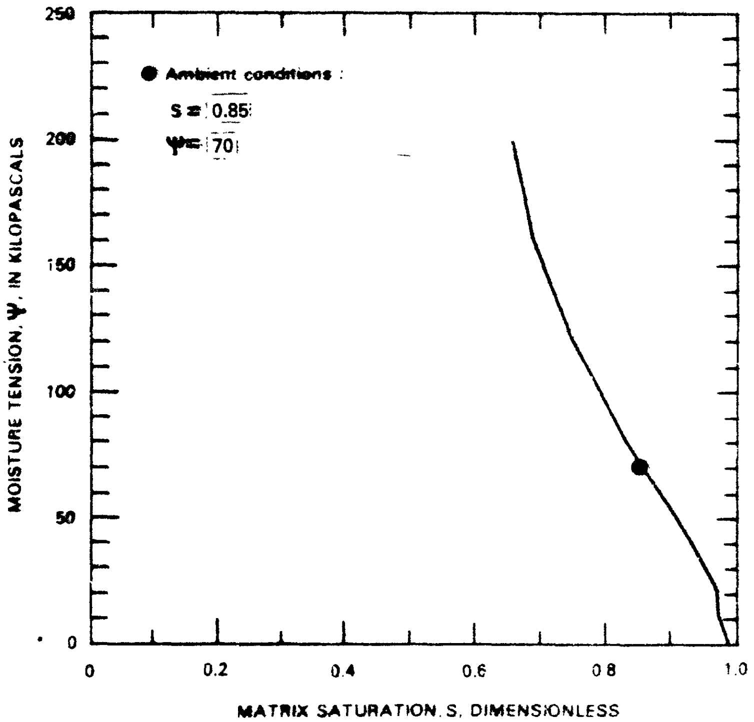

Figure 11.--Relation between saturation and moisture tension, core from test well USW H-1 at a depth of 219.2 meters (sample 8).

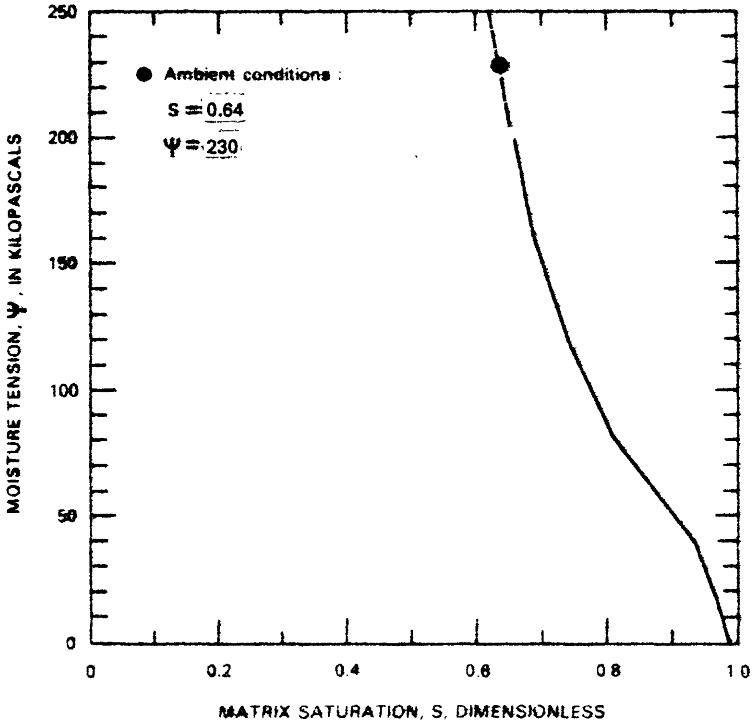

Figure 12.--Relation between saturation and moisture tension, core from test well USW H-1 at a depth of 221.4 meters (sample 9).

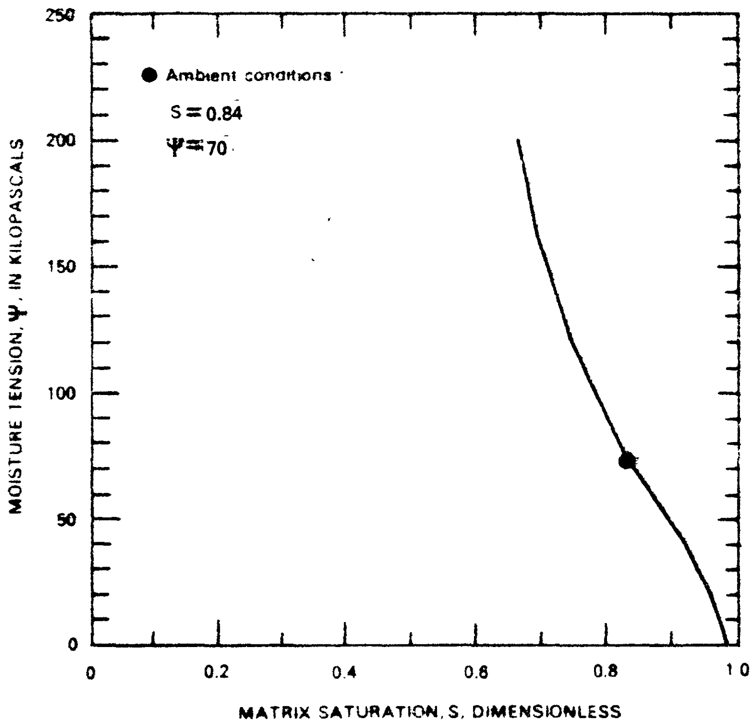

Figure 13.--Relation between saturation and moisture tension, core from test well USW H-1 at a depth of 222.1 meters (sample 10).

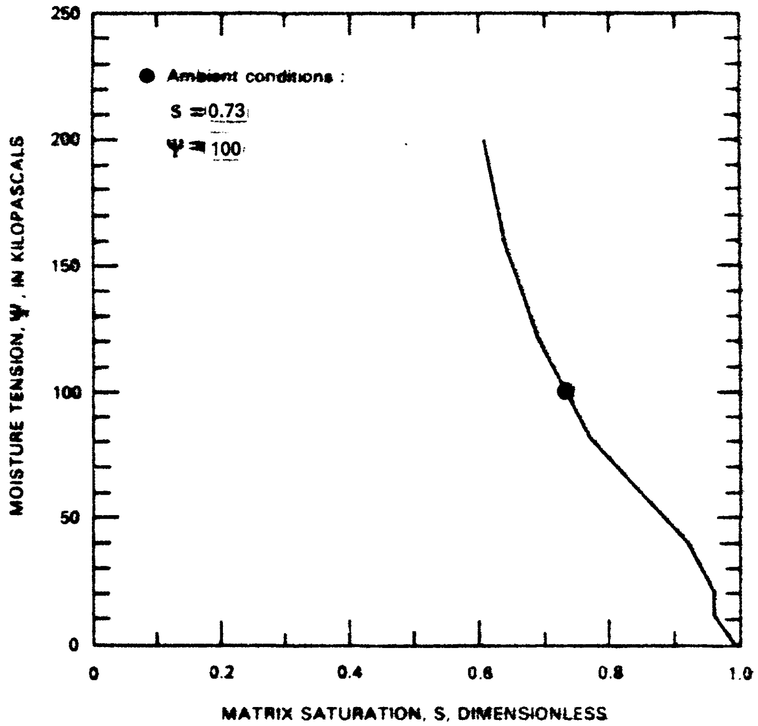

Figure 14.--Relation between saturation and moisture tension, core from test well USW H-1 at a depth of 225.6 meters (sample 11).

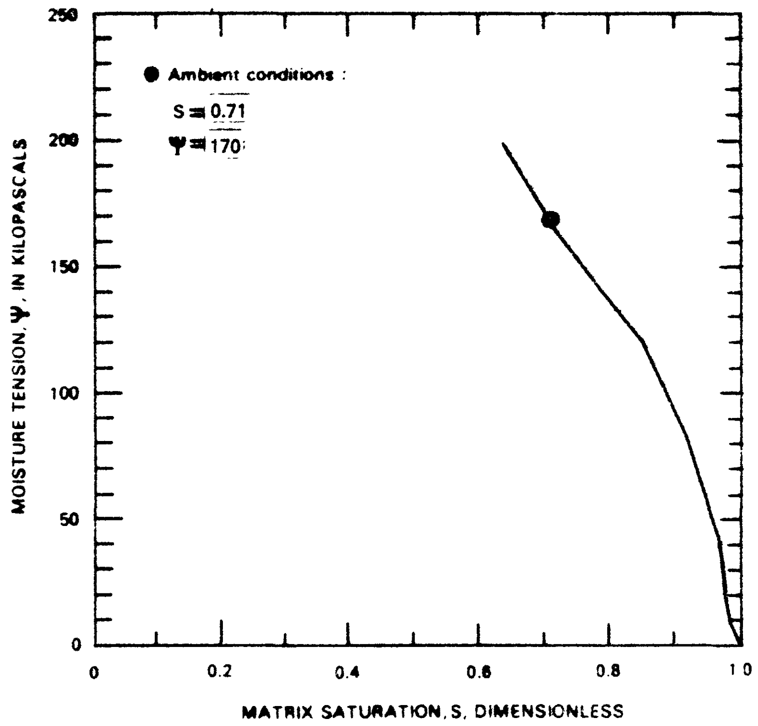

Figure 15.--Relation between saturation and moisture tension, core from test well USW H-1 at a depth of 390.4 meters (sample 12).

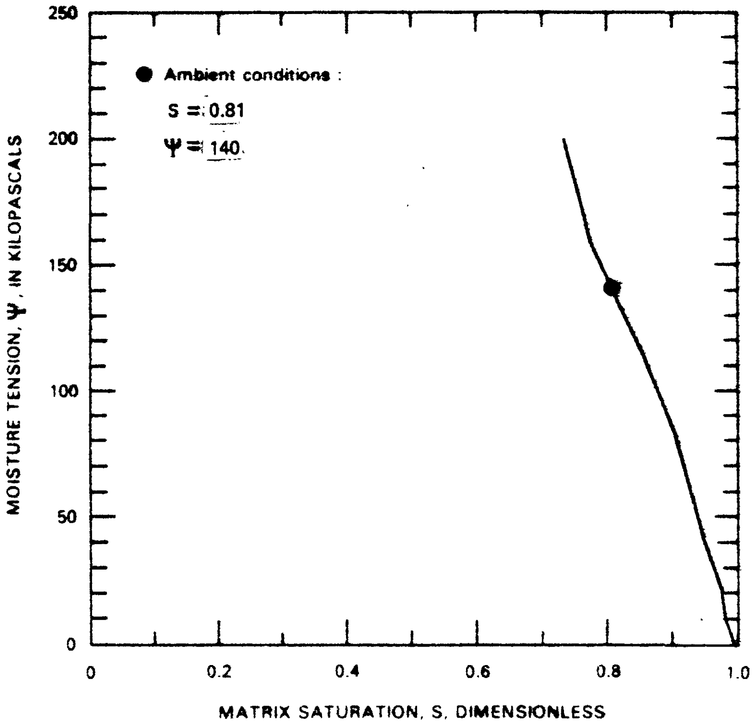

Figure 16.--Relation between saturation and moisture tension, core from test well USW H-1 at a depth of 390.6 meters (sample 13).

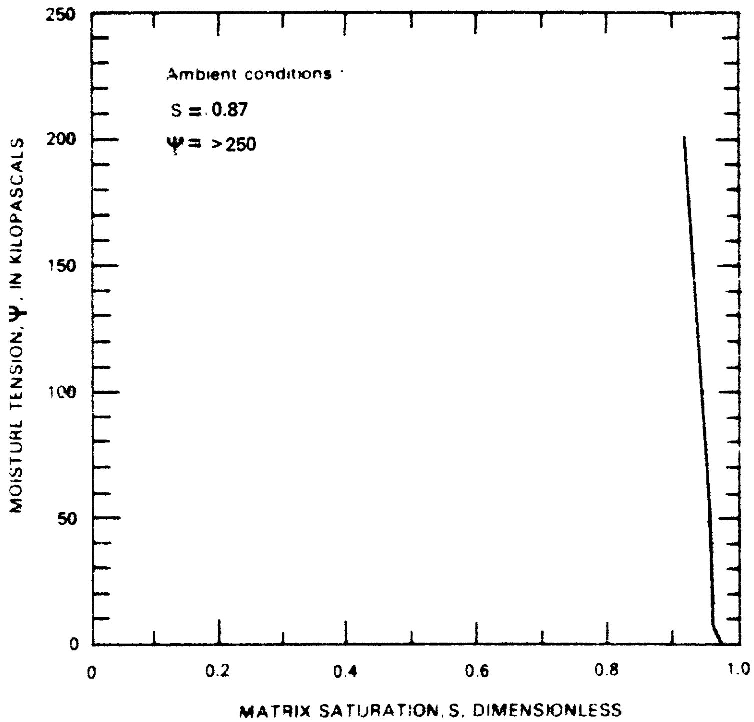

Figure 17.--Relation between saturation and moisture tension, core from test well USW H-1 at a depth of 397.9 meters (sample 14).

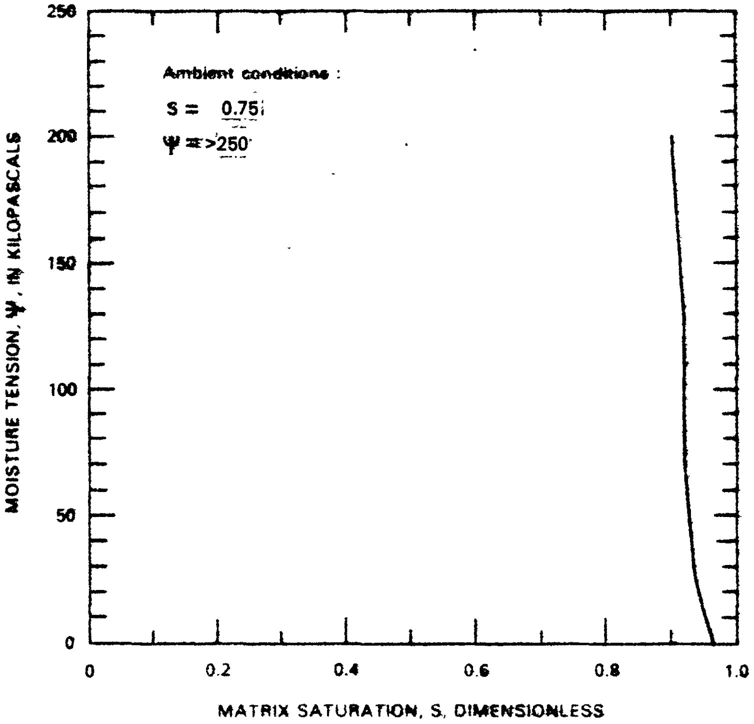

Figure 18.--Relation between saturation and moisture tension, core from test well USW H-1 at a depth of 398.7 meters (sample 15).

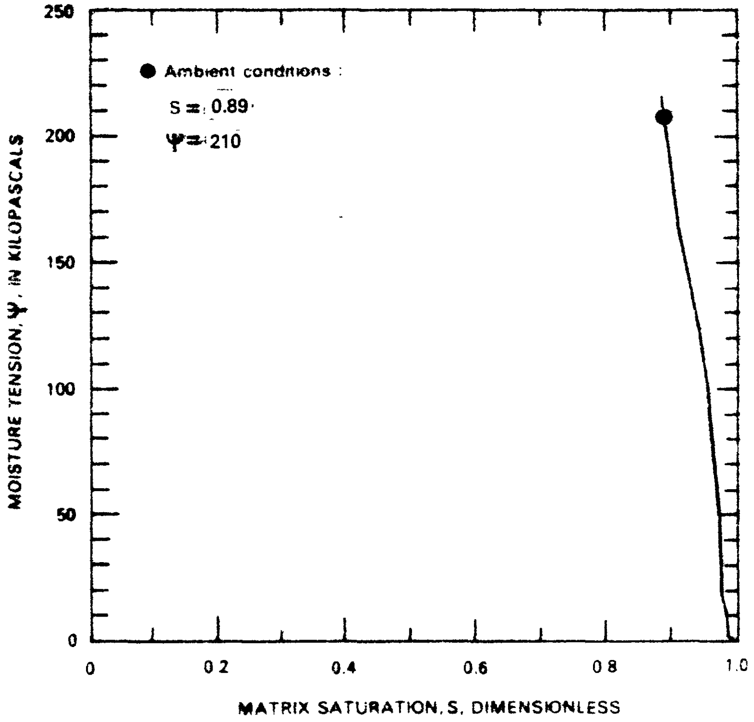

Figure 19.--Relation between saturation and moisture tension, core from test well USW H-1 at a depth of 405.4 meters (sample 16).

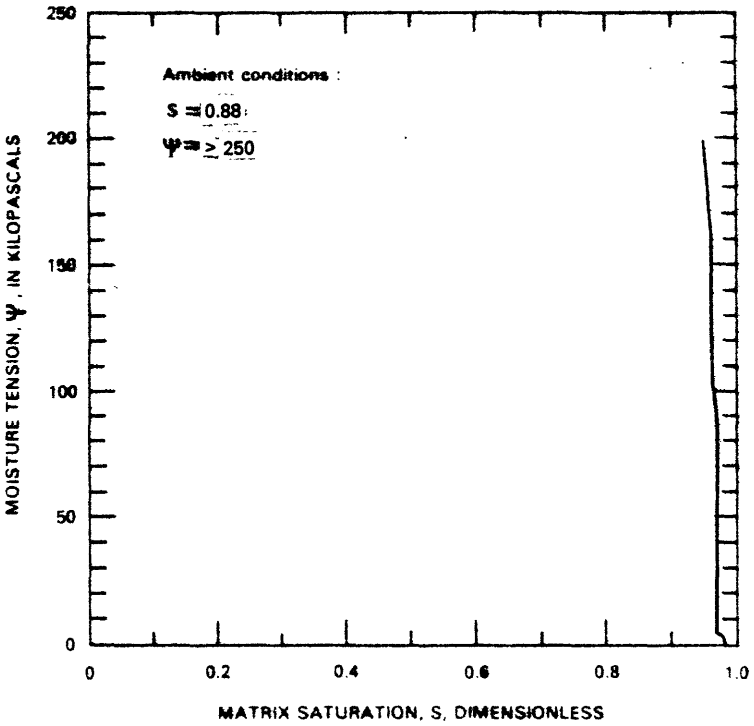

Figure 20.--Relation between saturation and moisture tension, core from test well USW H-1 at a depth of 405.8 meters (sample 17).

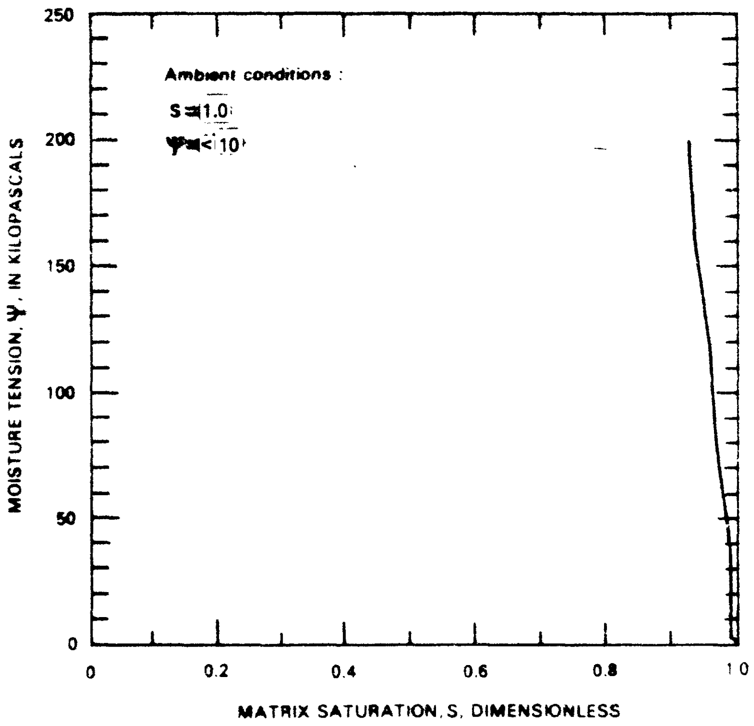

Figure 21.--Relation between saturation and moisture tension, core from test well USW H-1 at a depth of 530.7 meters (sample 18).

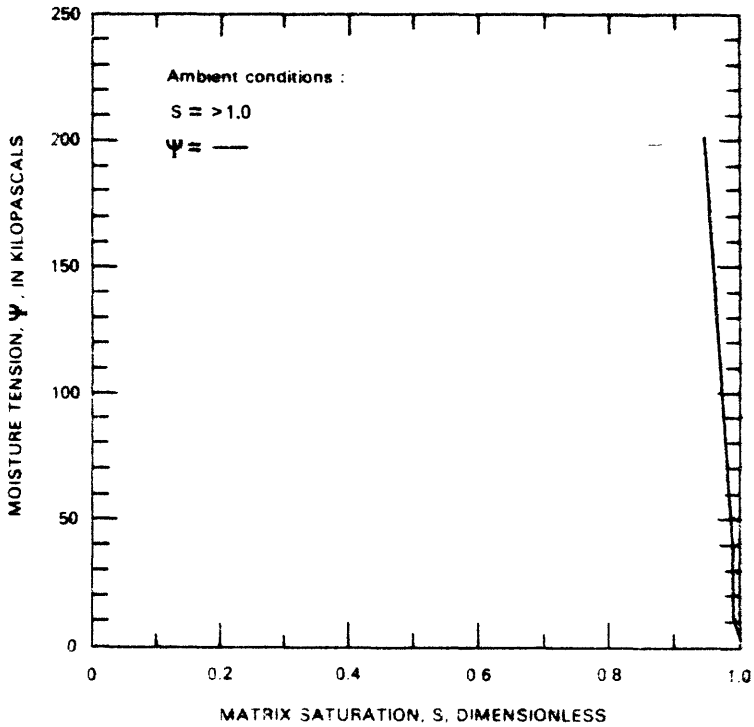

Figure 22.--Relation between saturation and moisture tension, core from test well USW H-1 at a depth of 532.8 meters (sample 19).

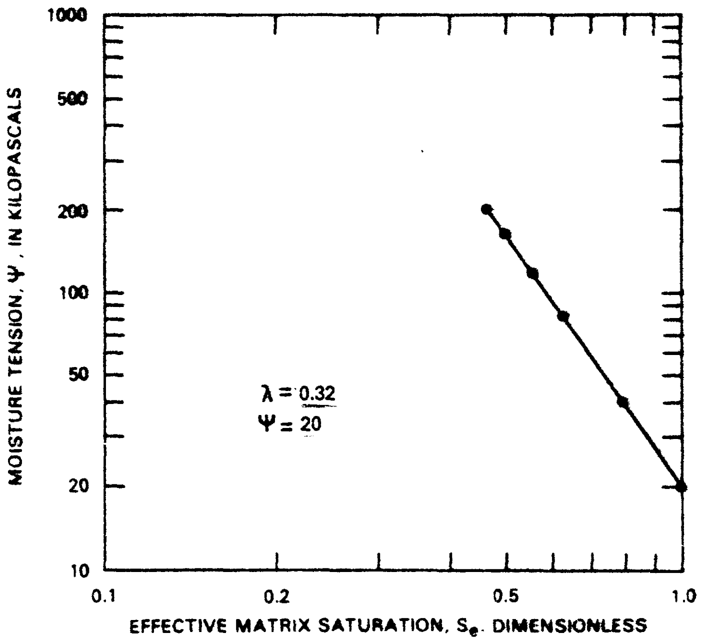

Figure 23.--Relation between the logarithm of effective matrix saturation and the logarithm of moisture tension, core from test well USW H-1 at a depth of 33.5 meters (sample 1).

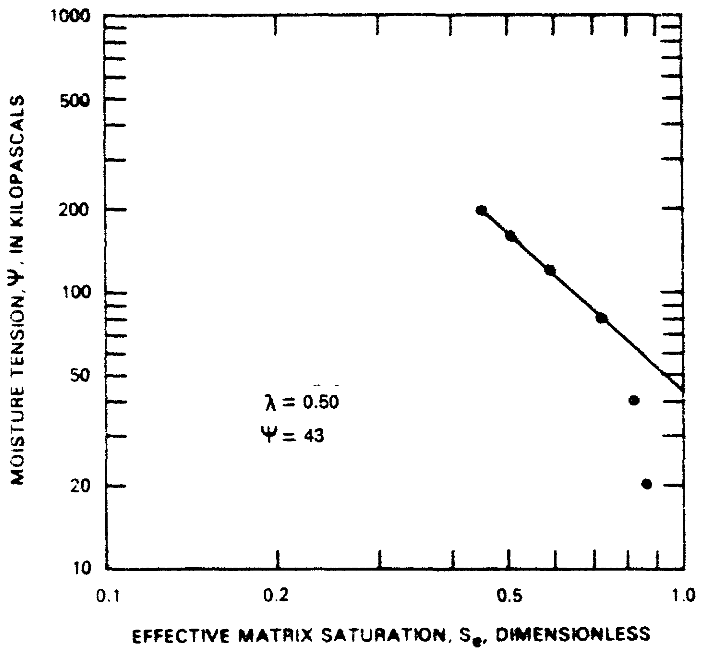

Figure 24.--Relation between the logarithm of effective matrix saturation and the logarithm of moisture tension, core from test well USW H-1 at a depth of 128.0 meters (sample 2).

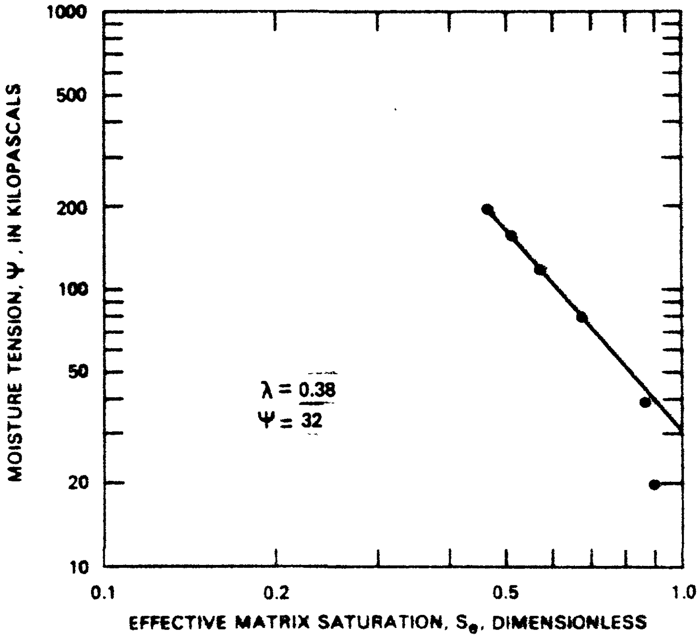

Figure 25.--Relation between the logarithm of effective matrix saturation and the logarithm of moisture tension, core from test well USW H-1 at a depth of 129.1 meters (sample 3).

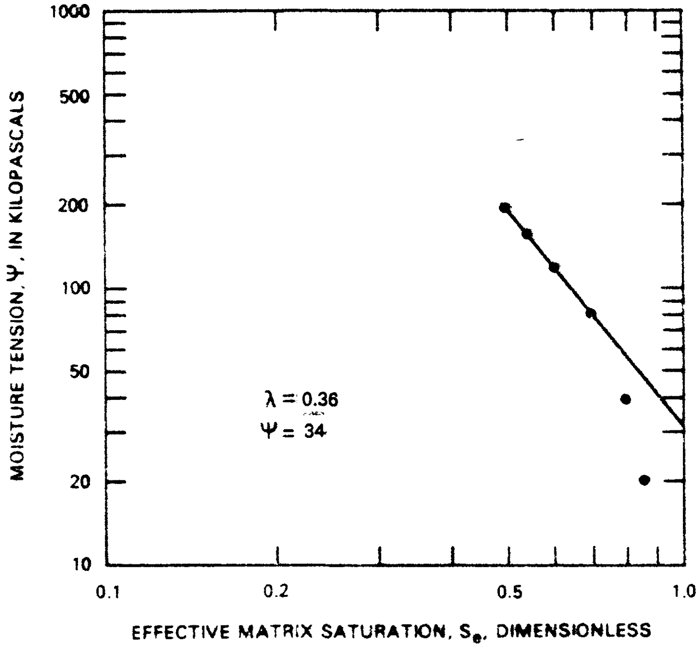

Figure 26.--Relation between the logarithm of effective matrix saturation and the logarithm of moisture tension, core from test well USW H-1 at a depth of 134.9 meters (sample 4).

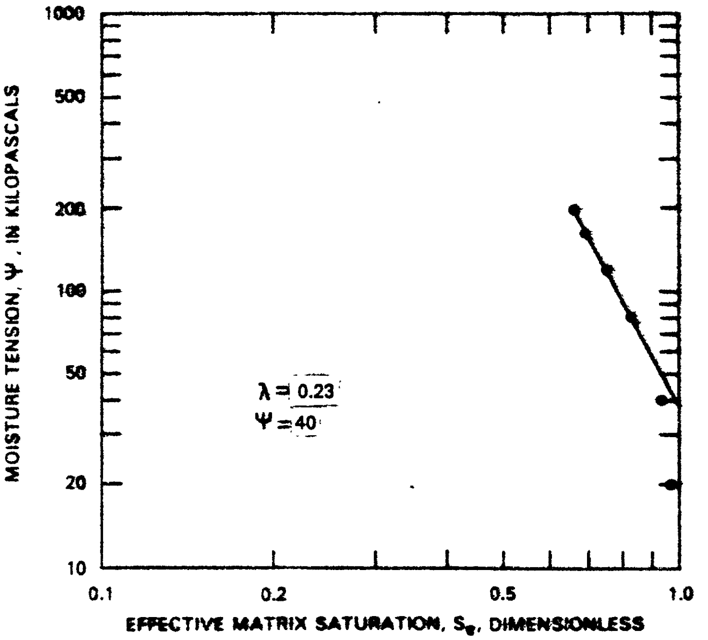

Figure 27.--Relation between the logarithm of effective matrix saturation and the logarithm of moisture tension, core from test well USW H-1 at a depth of 219.2 meters (sample 8).

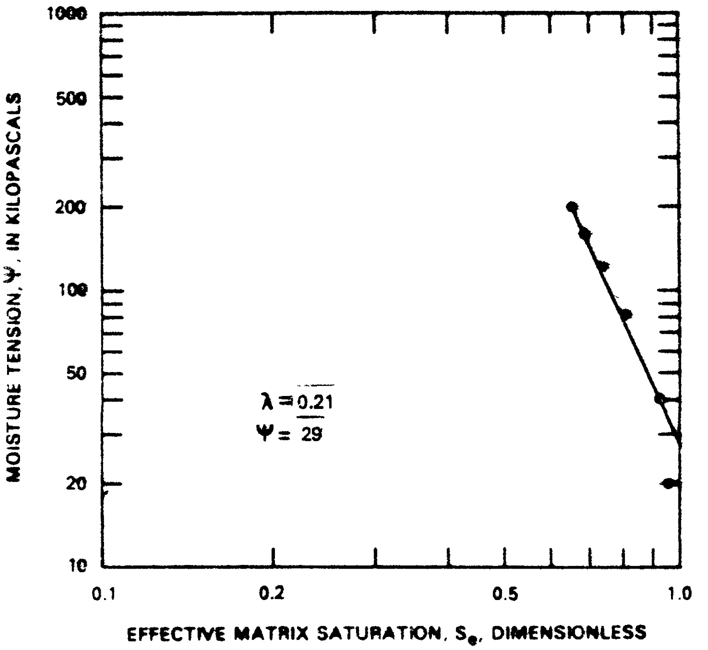

Figure 28.--Relation between the logarithm of effective matrix saturation and the logarithm of moisture tension, core from test well USW H-1 at a depth of 221.4 meters (sample 9).

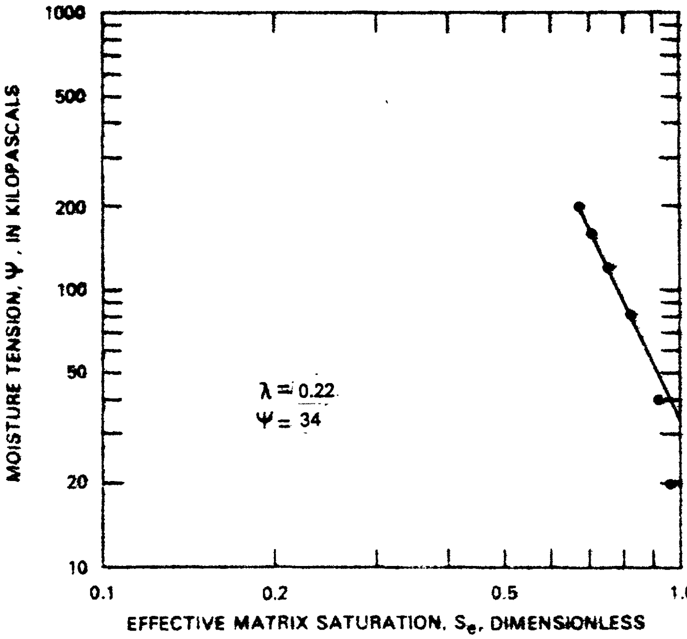

Figure 29.--Relation between the logarithm of effective matrix saturation and the logarithm of moisture tension, core from test well USW H-1 at a depth of 222.1 meters (sample 10).

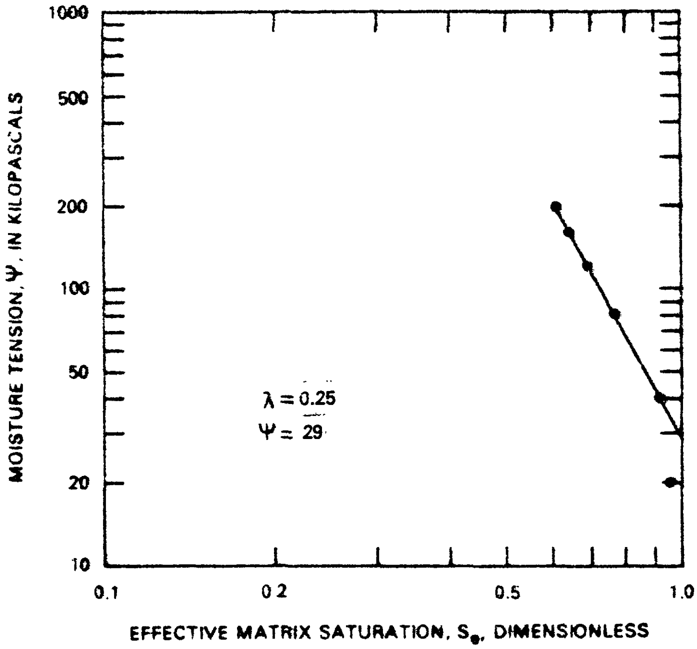

Figure 30.--Relation between the logarithm of effective matrix saturation and the logarithm of moisture tension, core from test well USW H-1 at a depth of 225.6 meters (sample 11).